EFFECT OF PROCESS PARAMETERS ON RESIDUAL STRESS AND THERMAL DEFORMATION IN VACUUM BRAZING OF INCONEL 617 PLATE CORE STRUCTURES

Ke WANG[1,2], Jinke LV[1,2], Shaoyang CHEN[1,2], Hao YANG[1,2], Tiange CHU[1,2], Qin ZHANG[1,2], Weijie CHEN[1,2]*

[1]School of Mechanics and Safety Engineering, Zhengzhou University, Zhengzhou 450001, China

[2]Key Laboratory of Process Heat Transfer and Energy Saving of Henan Province, Zhengzhou University, Zhengzhou 450002, China

* Corresponding author; E-mail: cwj135@gs.zzu.edu.cn

The compact plate heat exchanger is a key component in the solid oxide fuel cell combined heat and power system for waste heat recovery. To address issues such as high residual stress and poor weld quality after brazing, the high-temperature brazing process of a channel unit structure in the plate heat exchanger, designed for waste heat recovery, was simulated using the finite element software ABAQUS based on thermo-elasto-plastic theory. The residual stress distribution after brazing was obtained, and process parameters on residual stress were analyzed. The results show that the residual stress distribution of the channel structure is highly complex. The axial residual stress at the brazed joint between the plate and the spacer element at the channel inlet reaches a maximum of 313.3 MPa. The most severe plate deformation occurs at the brazed joint between the cold-side flow channel plate and the rectangular spacer element, reaching 0.107 mm, which is 286.6% of that at the same position on the hot side. With a decrease in brazing cooling rate, the residual stress gradually decreases. When the cooling rate is below 30 K/min, the internal residual stress of the channel structure can be effectively reduced. When BNi-2 nickel-based filler is used, the residual stress and flowability of the filler achieve an optimal balance.
Keywords: *Heat exchanger; Vacuum brazing; Thermal deformation; Residual stress*

1. Introduction

Compact plate heat exchangers (PHEs), distinguished by their superior thermal performance under high-temperature operating conditions, serve as critical components in solid oxide fuel cell (SOFC) systems for waste heat recovery, enabling efficient conversion of exhaust heat into electrical or thermal energy[1, 2]. At the heart of these exchangers lies a core structure comprising alternating hot and cold flow channels arranged in a stacked configuration. The fabrication precision of this core structure critically governs both the thermodynamic efficiency and long-term operational reliability of the entire heat exchange system[3].

The residual stresses induced by high-temperature brazing processes during core fabrication require urgent resolution. A mismatch in thermomechanical properties between the base metal and filler material generates significant residual stress fields at the weld interface during cooling[4, 5]. More critically, under actual operating conditions, these residual stresses interact with operational thermal stresses through nonlinear coupling effects, potentially triggering preferential microcrack propagation in stress concentration zones. While conventional heat treatment effectively mitigates residual stresses in macroscale structures, it proves severely limited for compact cores with micron-scale flow channels: Thermal gradients during heat treatment induce plastic deformation in thin-walled plates , causing irreversible geometric degradation of channel features[6]. This limitation underscores the imperative to investigate residual stress mitigation strategies that preserve microstructural integrity—a critical endeavor for ensuring the operational safety and longevity of compact plate heat exchangers.

In the past decade, numerous researchers have focused on analyzing the mechanical properties of heat exchanger structures after high-temperature brazing. Jiang et al. [7] investigated the residual stresses generated in the stainless steel plate-fin structure during the brazing process using three-dimensional finite element analysis. The results showed that the maximum residual stress occurs at the brazed joint of the plate-fin structure, indicating that the brazed joint is the weakest point of the entire structure. Zhou et al. [8] studied the distribution and optimization of residual stresses in plate-fin structures after brazing through finite element simulation, focusing on solidification cooling rates and assembly pressure. Li et al. [9] conducted a thermo-solid coupling simulation of the vacuum brazing process for titanium alloy plate-fin structures, discussing the temperature uniformity and residual stress distribution characteristics during brazing and elucidating the mechanism of the influence of holding time on the temperature field and residual stress during vacuum brazing. Ho-Seung Jeong et al. [10] used finite element analysis and experimental design to investigate the structural characteristics of brazed corrugated plates under temperature and pressure loads, focusing on the influence of design variables on stress levels, deformation behaviors, and the locations of maximum stress, and proposed an optimized design model. Wan et al. [11] proposed an isothermal solidification brazing method combined with an optimized post-bonding heat treatment strategy to improve the strength and ductility of brazed joints and homogenize the microstructure, thus enhancing the mechanical performance and energy efficiency of SOFC plate-fin heat exchanger joints.

In summary, domestic and international researchers have primarily focused on the brazing residual stress of plate-fin structures in heat exchangers, with relatively little research on the distribution and optimization of brazing residual stresses in compact plate heat exchangers. Previous studies have shown that under high-temperature conditions, stress concentration is most likely to occur at the brazed joints of heat exchangers, leading to cracking and failure [12]. Therefore, a systematic study of the effects of the brazing process on the post-weld residual stress in plate heat exchangers, as well as the impact of residual welding stress on the reliability of welded components, has substantial theoretical and practical value. In this paper, finite element simulation is used to study the thermal deformation and residual stress distribution of a compact plate heat exchanger, which is applied to waste heat recovery in SOFC systems after brazing. The influence of cooling rate and filler type on residual stress is analyzed, providing a basis for optimizing the brazing process and reducing residual stress.

2. Finite element modeling and analysis

2.1. Vacuum brazing channel structure

The overall structure of the compact plate heat exchanger used for SOFC waste heat recovery is shown in Fig. 1 (a), which is a sandwich structure composed of a series of plates and spacer elements.

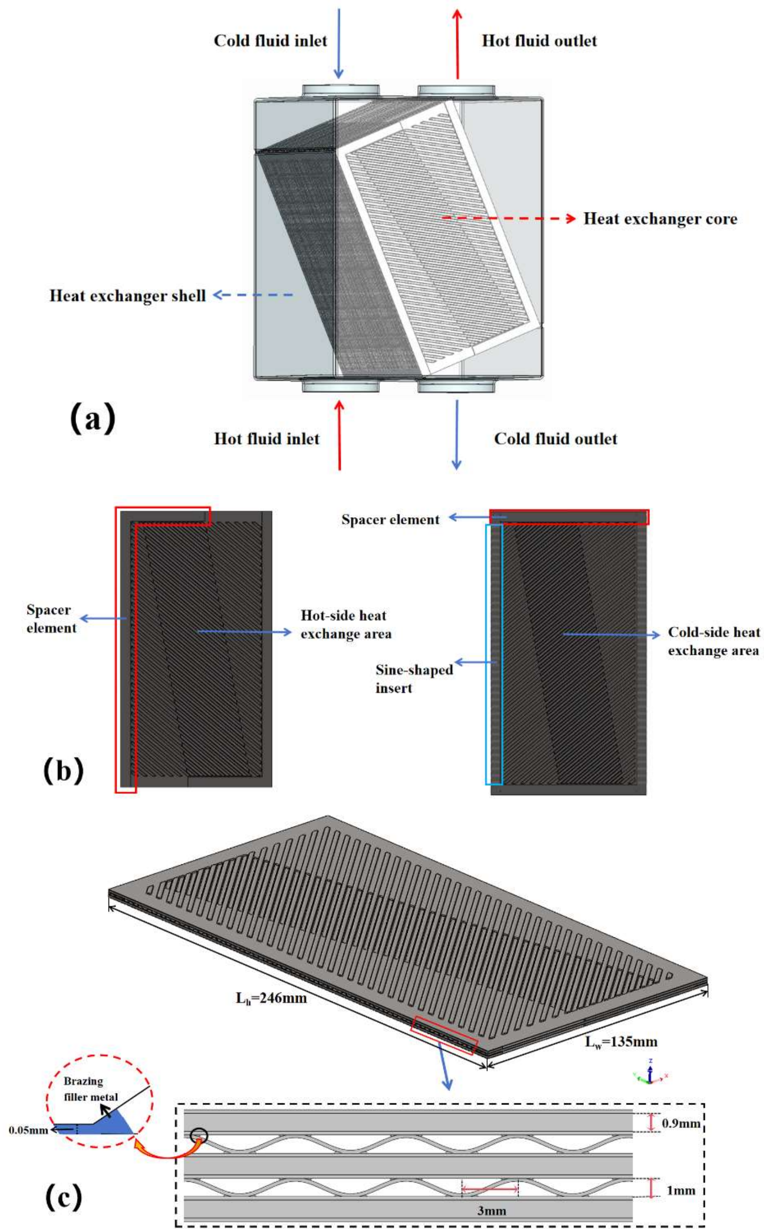

Figure 1. Core structure and flow channel unit of heat exchanger; (a) compact plate heat exchanger overall model; (b) structural diagram of hot and cold side flow channels; (c) sectional drawing and related dimensions of heat exchanger

These components are assembled into a complete core and then vacuum brazed to form an integrated unit. Each flow channel unit consists of two heat exchange plates clamping a spacer element, with brazing foils placed between the plates and the spacer element. The structural distribution of the hot-side and cold-side flow channels is illustrated in Fig. 1(b), where the shapes of the spacer elements are different between the flow channels. The hot-side flow channel is equipped with sinusoidal inserts at the inlet and outlet for flow guiding, and the hot and cold fluids flow across each other between the plates. The cross-sectional view of the flow insert is shown in Fig. 1(c), where the heights of both the hot-side and cold-side flow channels are 1 mm, the plate thickness is 0.2 mm, the spacer element thickness is 0.9 mm, and the brazing gap is controlled to 0.05 mm.

Table 1. Chemical composition of Inconel 617 and nickel-based brazing fillers (mass fraction, %)

material	Cr	Co	Nb	Al	C	Ti	Mo	Fe	Ni	Si	B
Inconel617	23.00	12.00	0.20	1.50	0.05	0.20	9.00	0.90	Bal.	-	-
BNi-1	14.00	-	-	-	0.75	-	-	4.50	73.56	4.00	3.10
BNi-2	7.00	-	-	-	0.06	-	-	3.00	82.34	4.50	3.10
BNi-4	-	-	-	-	0.06	-	-	1.50	93.09	3.50	1.85

Table 2. Thermal and mechanical properties of Inconel617 and BNi-X

Material	Temperature (K)	CET (10^{-6} K^{-1})	Conductivity (Wm^{-1}K^{-1})	Specific heat (JKg^{-1}K^{-1})	E (GPa)	μ (-)	Yield strength (MPa)
Inconel 617	293	11.6	13.4	419	211	0.3	285
	673	13.6	19.3	515	188	0.3	210
	1173	15.8	27.1	636	149	0.3	185
BNi-1	293	1.30	23.84	473	215.5	0.292	534
	673	1.61	27.54	587	193.9	0.301	458
	1173	2.10	31.68	1060	119.6	0.330	371
BNi-2	293	1.35	25.59	469	205.1	0.296	424
	673	1.68	29.18	577	183.2	0.306	368
	1173	2.13	33.58	1161	127.6	0.328	255
BNi-4	293	1.36	17.21	456	202.4	0.284	399
	673	1.69	18.87	544	181.8	0.292	324
	1173	2.16	25.79	2190	103.5	0.329	221

The material selected for the heat exchanger is Inconel 617 alloy, which meets the requirements of the heat exchanger due to its high creep rupture strength, excellent corrosion resistance, superior high-temperature oxidation resistance, and creep resistance. Nickel-based filler metals BNi-1, BNi-2, and BNi-4 were used for brazing, and their chemical compositions are shown in Tab. 1. The temperature-dependent material properties are required to finish the finite element analysis. Some data are shown in Tab. 2. Here, CET represents the coefficient of thermal expansion, E denotes the elastic modulus, and μ stands for Poisson's ratio. The selection of BNi-1, BNi-2, and BNi-4 nickel-based brazing fillers for this study was driven by their distinct thermodynamic properties and documented industrial applicability in plate-fin heat exchanger manufacturing. These fillers exhibit varying boron and chromium compositions—critical elements governing interfacial diffusion kinetics and residual stress generation[13]. A uniform peak temperature of 1373 K was applied for BNi-1, BNi-2, and BNi-4 filler metals. While actual liquidus temperatures vary between 1272-1339 K for these alloys, maintaining isothermal conditions enables direct comparison of material property effects.

2.2. Geometric model and mesh division

Due to the fact that the weakest points and potential failure locations of the heat exchanger structure under high-temperature operating conditions are at the brazed joints, these joints become the primary focus of the research and analysis. To reduce the complexity of the simulation and save analysis time, the corrugation of the plates can be simplified during finite element simulations. As shown in Fig. 1, the core structure exhibits symmetry, periodicity, and complexity. Therefore, the analysis model in the simulation adopts a periodic unit, and the finite element software Abaqus is used to establish the computational model. Three flow channel units (two cold-side channels and one hot-side channel) are selected as the study objects, as illustrated in Fig. 2.

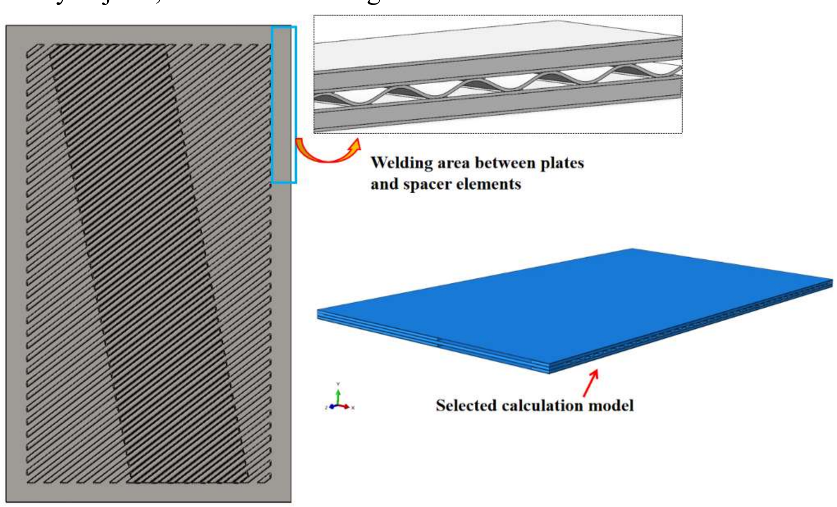

Figure 2. Brazing of heat exchanger and analysis calculation model

Due to the significant residual stress gradient in the weld and the adjacent base material, which can easily lead to stress concentration, mesh refinement was applied to the weld and the surrounding base material to improve the accuracy of the model calculations. In contrast, relatively coarser meshing was used in regions far from the weld, as illustrated in Fig. 3, which shows the mesh division of the finite element model. The final total number of computational mesh elements is 226,019.

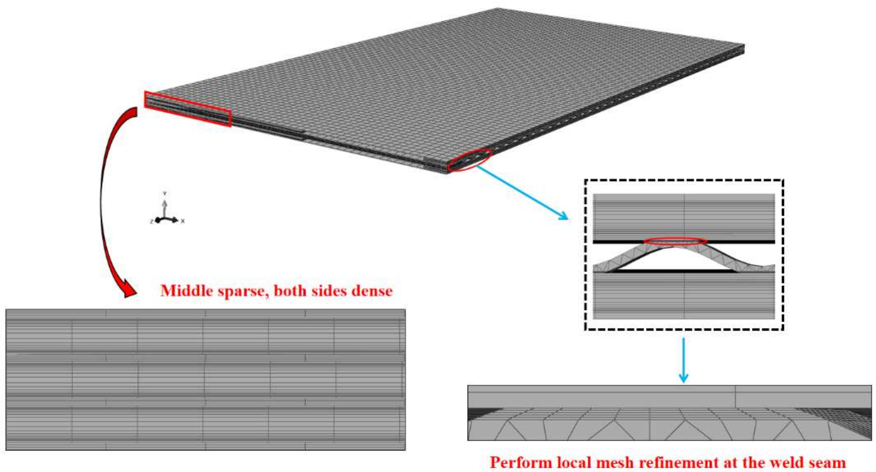

Figure 3. Mesh division diagram of finite element model

2.3. Thermo-mechanical coupling model and boundary conditions

After establishing the three-dimensional nonlinear finite element model for brazing the heat exchanger plates, a thermo-mechanical coupling approach was used for finite element analysis based on thermo-elasto-plastic theory[14]. The model assumes an absolute vacuum (0 Pa) within the brazing furnace chamber. While industrial vacuum levels typically range from 10^{-3} to 10^{-5} mbar, this simplification eliminates the complexities of convective heat transfer while maintaining the accuracy of radiation-dominated thermal modeling. The specific temperature variation inside the furnace is illustrated in Fig. 4. As can be seen from the figure, the temperature change throughout the brazing process involves eight distinct steps: (1)Heating for 30 minutes, raising the temperature from 293 K to 773 K; (2)Holding at 773K for 30 minutes; (3)Heating for 25 minutes, raising the temperature from 773 K to 1173 K; (4)Holding at 1173 K for 30 minutes; (5)Heating for 15 minutes, raising the temperature from 1173 K to 1373 K; (6)After 30 minutes of brazing diffusion at 1373 K, the brazed joints are formed; (7)Nitrogen cooling, reducing the furnace temperature from 1373 K to 473 K; (8)Natural cooling for 90 minutes, lowering the specimen temperature to room temperature.

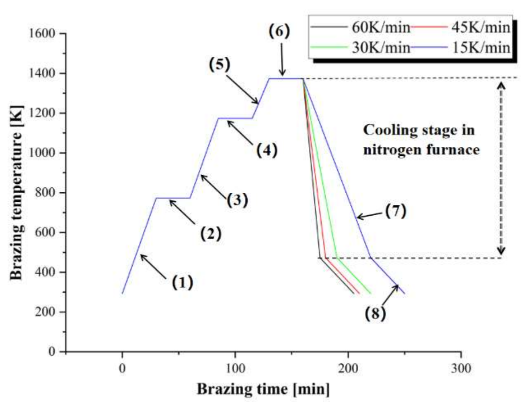

Figure 4. Furnace temperature control curve

During the vacuum brazing process, the overall temperature field distribution inside the furnace undergoes significant changes over time. Therefore, the temperature field during vacuum brazing represents a typical nonlinear transient heat conduction problem. The primary heat transfer processes occurring in the vacuum brazing furnace include thermal radiation between the heating elements and the workpiece surface, as well as heat conduction within the workpiece itself. There is no convective heat transfer between the workpiece and the surrounding environment.

When conducting finite element analysis using a thermo-mechanical coupling approach, the heat transfer analysis must first consider the radiative heat transfer within the flow channel structure of the vacuum furnace. The formula is given as follows：

$$q = \varepsilon\sigma(\theta^4 - \theta_0^4) \tag{1}$$

In the formula, q represents the radiative heat flux per unit area of the surface; ε is the surface emissivity (which is temperature-dependent); σ is the Stefan-Boltzmann constant; and θ is the temperature.

When analyzing radiation heat transfer in the channel space enclosed by plates and spacer elements, cavity radiation calculations are required. Thus, radiation from the furnace heater to the external surfaces of the brazing unit and the internal cavity channels is included as radiation flux boundary conditions in the finite element analysis. The radiation flux entering the cavity surface per unit area is given by:

$$q_i^c = \frac{\sigma\varepsilon_i}{A_i}\sum_j \varepsilon_j \sum_k F_{ik} C_{kj}^{-1}((\theta_j - \theta^2)^4 - (\theta_i - \theta^2)^4) \tag{2}$$

$$C_{ij} = \delta_{ij} - \frac{(1-\varepsilon_i)}{A_i} F_{ij} \tag{3}$$

where F is the surface view factor, and C is the surface reflection matrix, which depends on the distance and orientation of the surfaces.

The temperature variations obtained from the heat transfer analysis are applied as thermal loads in the subsequent mechanical analysis. The pressure applied by the clamping fixture is uniformly distributed on the upper surface of the structure. Based on the thermo-elasto-plastic response of the structure, the residual stress and thermal deformation of the structure can then be determined.

The lower surface of the plate (XOZ) is positioned on a fixed support, preventing displacement in the Y-direction. Therefore, a displacement constraint is applied in the Y-direction to the lower surface of the plate. The contact surfaces between the plates, spacer elements, and brazing filler metal are restricted from undergoing any relative displacement, and they must remain in contact along the normal direction. Since heat and mechanical forces are transmitted across these contact surfaces, tied contact conditions are applied to all interfaces. To prevent rigid body motion during the simulation, displacement constraints in the X- and Z-directions are applied to both the upper and lower surface center nodes of the plate along this central axis. The simulation considered the effects of temperature on the material's elastic modulus, thermal expansion coefficient, yield strength, and Poisson's ratio. The model assumes a geometrically perfect filler layer with uniform thickness, neglecting the effects of brazing filler flow and interfacial diffusion.

Using the simulation method adopted in this study, the model from reference [15] was analyzed, and the residual stress distribution along the path is shown in Fig. 5. The simulation results in this study are consistent with the trend observed in the reference, with an error of less than 75 MPa compared to the experimental residual stress values. Therefore, it can be concluded that the simulation method employed in this study provides results with a high level of accuracy.

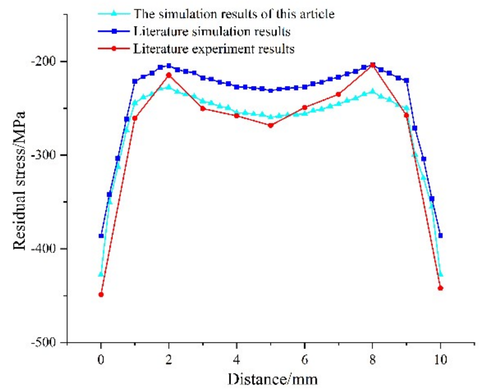

Figure 5. Comparison of the simulated values in this study with the values from the reference

3. Results and Discussion

3.1. Changes in brazing temperature field

Points A, B, and C were established, as shown in Fig. 6, to investigate the temperature variation at different positions from the interior to the exterior during the brazing process. From the figure, it can be seen that the cooling patterns of all three points are essentially identical. Since Point A is located on the surface of the specimen, it is less affected by heat conduction from the specimen and radiation from the cavity, thus reaching the same temperature earlier than Point C. It can be inferred that as the number of flow channel layers increases, the time difference for reaching the brazing temperature between the interior and exterior becomes more pronounced. Therefore, special attention must be given to controlling the brazing time of multilayer core structures to ensure adequate diffusion bonding of internal joints.

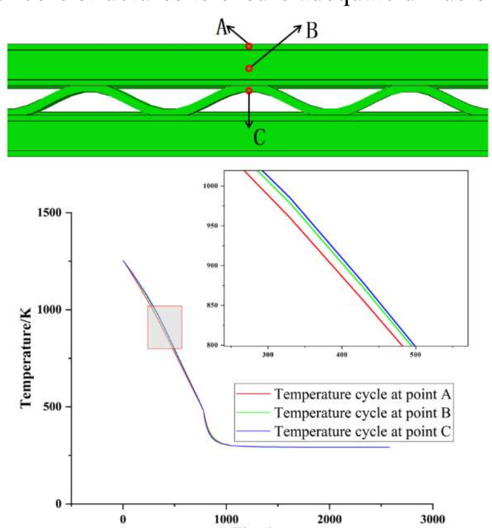

Figure 6. Comparison of the simulated values in this study with the values from the reference

The temporal variation of the temperature field in the hot runner heat exchange plate during the brazing process is illustrated in Fig. 7. It can be observed from the figure that the maximum temperature difference in the flow channel during brazing reaches 20.2 K, with the lowest temperature points primarily located at the corners. The significant temperature difference at the brazed joints between the plates and spacer elements is one of the main causes of high residual stress.

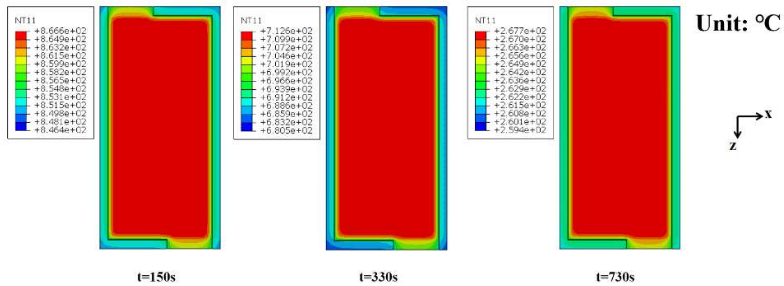

Figure 7. Comparison of the simulated values in this study with the values from the reference

3.2. Deformation after brazing

The typical characteristic of deformation in the flow channel structure is the shrinkage and distortion of the heat exchange plates. The deformation of the plates under two process conditions (filler: BNi-2; cooling rate: 60 K/min) is shown in Fig. 8. During the brazing process, a significant temperature gradient was generated at the plate edges due to radiation within the flow channels, inducing thermal

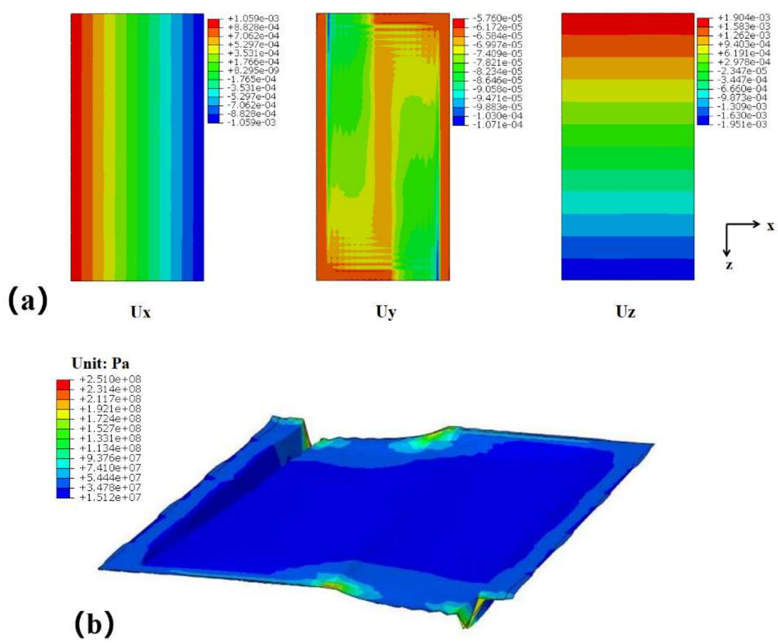

Figure 8. Deformation of the board; (a) deformation of the board in three directions; (b) cold measurement of channel plate deformation (deformation factor: 100)

stress. Concurrently, the contact between the plate ends and spacer components restricted their free thermal expansion and contraction, leading to compressive stress during the cooling phase. The combined effect of these factors resulted in negative deformation along the Y-direction at both ends of the plate. The most severe plate deformation occurs at the fillet weld of the cold-side flow channel, with an axial deformation reaching 0.107 mm, which is 286.6% of the deformation at the same position on the hot-side plate. This deformation changes the shape of the flow channel inlets and outlets, potentially causing uneven heat transfer between the hot and cold fluid channels, which can lead to reduced heat exchange efficiency during actual operation.

3.3. Distribution of residual stresses in brazing

The residual stress distribution of the heat exchange plates after brazing is shown in Fig. 9. The selected three paths at the brazed joints between the filler metal and base material are presented in Fig. 10, along with the stress distribution along these paths. The maximum stress in all three primary directions occurs in the brazed joint region. Among them, the maximum value of σ_y, perpendicular to the joint interface, reaches 313.3 MPa, even exceeding the yield strength of the base material (σ_s = 285 MPa). Both Path 1 and Path 2 exhibit significant stress gradients at their ends, with the overall residual stress along Path 2 being higher than that along Path 1. This is because Inconel 617 alloy, compared to BNi-2, possesses better plasticity, allowing plastic deformation to alleviate stress concentration.The additional stress peak observed along Path 2 arises from stress concentration at the interfacial region between the sinusoidal insert and the rectangular spacer component, induced by thermally-driven deformation mismatches during the brazing thermal cycle. Path 3 exhibits the highest and most complex residual stress, with multiple stress gradients formed. The high residual stress at the brazed joint between the flow insert and the plate increases the susceptibility to cracking, potentially leading to failure under the combined effects of complex loading and corrosion.

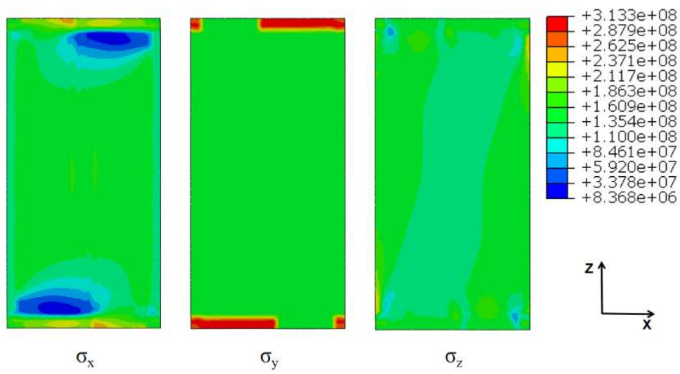

Figure 9. Residual stress distribution of the plates under two process conditions (filler: BNi-2; cooling rate: 60 K/min)

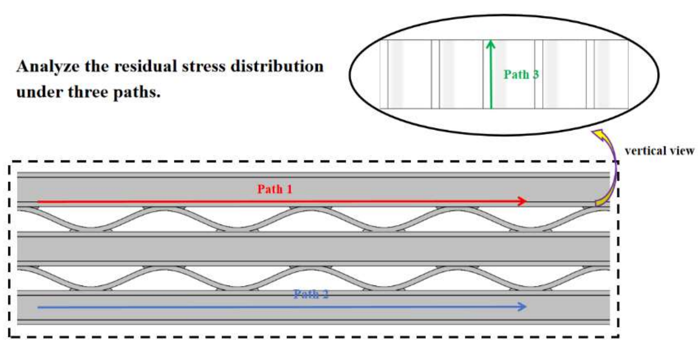

Figure 10. Selection of residual stress path for brazed joints

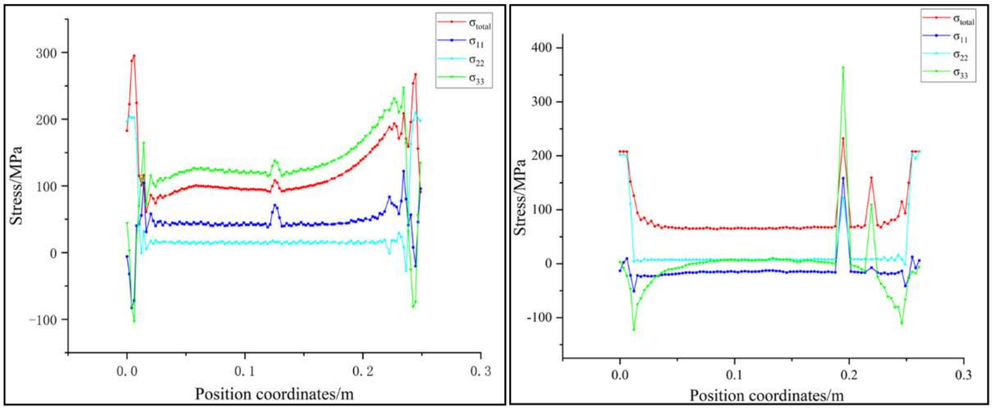

Figure 11. Stress distribution curve for path 1 (Left) and path 2 (Right)

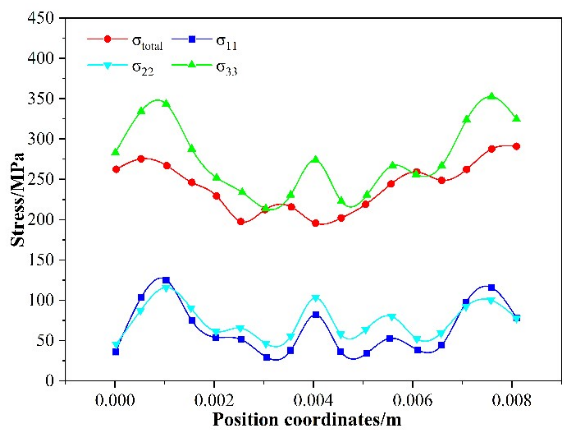

Figure 12. Stress distribution curve under path 3

3.4. The effect of brazing cooling rate on residual stress

During the brazing process, a nitrogen-assisted accelerated cooling protocol was implemented to rapidly reduce the global temperature from 1373 K to 473 K. This thermal treatment protocol aims to preserve the elevated-temperature plasticity, toughness, and machinability of the brazed joint metal at room temperature.The brazing cooling rate is an important parameter affecting the performance of brazed joints. In this study, cooling rates of 60 K/min, 45 K/min, 30 K/min, and 15 K/min were selected, with brazing conducted using BNi-2 filler, to investigate the effect of different cooling rates on brazing-induced thermal deformation and residual stress.

The furnace temperature control curves under different brazing cooling rates in the vacuum brazing furnace are shown in Fig. 4, while the comparison of residual stresses under different cooling rates is illustrated in Fig. 13. As seen in the figure, the larger the cooling rate, the higher the maximum residual stress and the greater the axial displacement deformation of the plate. The effect of cooling rate on residual stress is primarily due to the high temperature gradient that occurs at high cooling rates during the cooling process, which leads to larger residual stresses. When the cooling rate decreases from 60 K/min to 30 K/min, the maximum residual stress drops from 313.3 MPa to 98.7 MPa, a reduction of 68.5%. Further reducing the cooling rate results in only minor changes in residual stress, indicating that an optimal cooling rate is around 30 K/min. The residual stress distribution curves along a selected path for different cooling rates are shown in Fig. 14. The brazing residual stress exhibits a symmetric distribution, with the center point of the weld seam between the plate and spacer element as the symmetry center. The residual stress reaches its minimum at the midpoint of the weld seam and its maximum at both ends, with significant stress gradients at the weld seam ends. As the brazing cooling rate decreases, the residual stress also decreases, and the differences in residual stress between different cooling rates diminish. Therefore, when the brazing rate falls below a certain value, the residual stress at the weld seam between the spacer element and the plate will approximate a constant value. Consequently, the lower the brazing cooling rate, the lower the risk of weld seam fracture in the flow channel structure due to residual stresses.

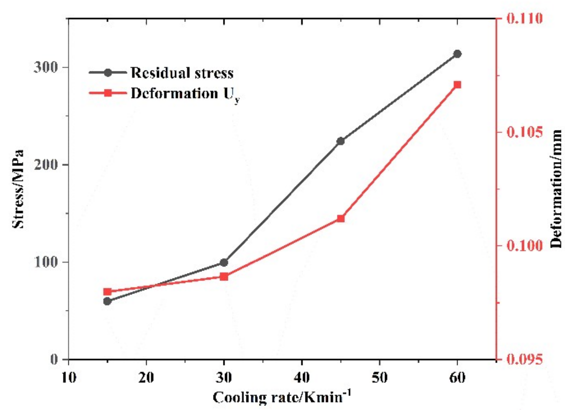

Figure 13. Maximum axial residual stress values and axial deformation under different cooling rates

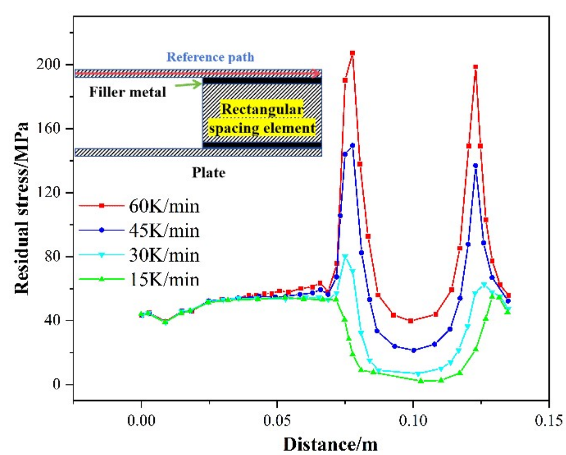

Figure 14. Residual stress distribution along the selected path

3.5. The effect of different brazing materials on residual stress

Nickel-based brazing fillers with different silicon and boron contents significantly affect the microstructure, mechanical properties, and strength of brazed joints. As shown in Tab. 3, different fillers have a notable impact on the residual stress of brazed joints. BNi-1 contains higher levels of boron and chromium, resulting in greater strength and hardness. During the brazing process, the rapid diffusion of these elements leads to high residual stresses, making the joints more susceptible to the formation of brittle borides. In contrast, joints brazed with BNi-4 exhibit lower residual stresses, which reduces the stress gradient at the interface and improves the overall joint quality. However, due to its lower boron content, BNi-4 has poorer flowability, making it unsuitable for brazing complex components. BNi-2, on the other hand, achieves a good balance between low residual stress and good flowability[16]. Therefore, from the perspective of structural strength and weld quality, BNi-2 is more suitable for brazing Inconel 617 plate heat exchangers.

Table 3. Maximum residual stress and deformation of the structure for different brazing filler metals

BNi-x	σ_x（MPa）	σ_y（MPa）	σ_z（MPa）	U（total）（mm）
BNi-1	246.13	374.1	108.06	3.208
BNi-2	236.01	313.3	88.48	2.609
BNi-4	240.02	307.1	94	3.017

4. Conclusions

In this study, a thermo-mechanical coupling model of a compact plate heat exchanger was established, focusing on the deformation of the plates and spacer elements after brazing, as well as the residual stress distribution. The effects of cooling rate and different brazing materials on residual stress were also analyzed. The main conclusions are as follows:

1. The maximum deformation of the plate occurs at the fillet weld of the joint between the cold-side flow channel inlet and the spacer element, with an axial deformation of 0.107 mm, which is 286.6% of that at the same position on the hot-side flow channel. This location is highly prone to cracking under service conditions. Therefore, more attention should be given to the brazed joint near the flow channel inlet.
2. The maximum stress in all three principal directions occurs in the brazed joint region, with the maximum value perpendicular to the joint interface reaching 313.3 MPa, exceeding the yield strength of the base material.
3. The faster the brazing cooling rate, the greater the residual stress in the structure. As the cooling rate decreases, the difference in residual stress gradually diminishes. When the cooling rate is reduced from 60 K/min to 30 K/min, the maximum residual stress decreases by 68.5%.
4. Different nickel-based fillers have a significant impact on residual stress and deformation. BNi-2 achieves an optimal balance between low residual stress and good flowability. Compared to BNi-1, the axial residual stress is reduced by 16.3%, and compared to BNi-4, the total deformation is reduced by 13.5%.

In this study, BNi-1, BNi-2, and BNi-4 brazing filler metals were selected to analyze the influence of different chemical compositions, particularly boron and chromium content, on residual stresses in brazed joints. Similarly, BNi5 and BNi-7, which are widely used in brazing applications and serve as critical materials under specific high-temperature conditions, demonstrate potential advantages in high-temperature creep resistance. These alloys will be considered in future research to expand the scope of investigation and further explore their performance characteristics.

The flow and diffusion of the brazing filler metal and brazing temperature are critical factors affecting the mechanical properties of brazed joints. While this study focuses on thermodynamic properties to analyze residual stresses, future work will systematically investigate the effects of filler metal flow, diffusion, and temperature gradients on residual stress formation.

References

[1] Khan, M. S., *et al.*, Numerical analysis of thermal performance of heat exchanger different plate structures and fluids, *Thermal Science, 26* (2022), 2, pp. 1151-1163

[2] Zhang, X., *et al.*, An additively manufactured metallic manifold-microchannel heat exchanger for high temperature applications, *Applied Thermal Engineering, 143* (2018), pp. 899-908

[3] Adamiec, J., Urbanczyk, M., The effect of the welding technology on the thermal performance of welded finned tubes used in heat exchangers, *Energies, 16* (2023), 3, pp. 101-112

[4] Ma, H. Q., He, B. X., Influence of brazed joints on stress of plate-fin structures in LNG heat exchanger, *Journal of Harbin Institute of Technology, 51* (2019), 02, pp. 172-178

[5] Du, X. W., *et al.*, Experimental analysis of key parameters of laser ion welding of honeycomb plate heat exchanger, *Thermal Science, 23* (2019), 5, pp. 2757-2764

[6] Chen, H., *et al.*, Finite element analysis of residual stresses and thermal deformation for brazing plate-fin structure, *Transactions of the China Welding Institution, 27* (2006), 11, pp. 29

[7] Jiang, W. C., *et al.*, Residual stress in brazed stainless steel plate-fin structure and its influencing factor, *Acta Metallurgica Sinica, 44* (2008), 1, pp. 105-111

[8] Zhou, G. Y., Tu, S. D., Research on Distribution and Optimization of Residual Stress in Brazed Plate Wing Structure, *Nuclear Power Engineering, 31* (2010), 04, pp. 101-105

[9] Li, Y., *et al.*, Thermal-fluid-solid coupling analysis of vacuum brazing process for a titanium alloy plate-fin structure, *Vacuum, 218* (2023), 3, pp. 132-147

[10]Jeong, H. S., *et al.*, Investigation into structural reliability of a brazed part in cross-corrugated plates, *International Journal of Precision Engineering and Manufacturing, 15* (2014), 2, pp. 251-258

[11]Wan, Y., *et al.*, Brazing manufacturing technology of plate-fin heat exchanger for solid oxide fuel cells, *International Journal of Hydrogen Energy, 48* (2023), 11, pp. 4456-4468

[12]Wan, Y., *et al.*, Creep damage and crack propagation behavior of printed circuit heat exchanger manufactured by diffusion welding: from material to structure, *Journal of Materials Research and Technology-Jmr&T, 27* (2023), pp. 1446-1460

[13]Chen, H., *et al.*, Study of Parameter Effects on Residual Stresses and Thermal Deformation of Brazed Plate-Fin Structure Using Finite Element Method, *Journal of Pressure Vessel Technology-Transactions of the Asme, 130* (2008), 4, pp. 1-6

[14]Ni, X. N., *et al.*, Thermodynamic study of molten pool during selective laser melting of alsi10mg alloy, *Thermal Science, 28* (2024), 6B, pp. 5231-5243

[15]Qiao, R. L., Long, W. M., Numerical simulation of residual stress in YG8/GH4169 dissimilar material brazed joints, *Transactions of the China Welding Institution, 45* (2024), 03, pp. 11-17

[16]Jang, J. S. C., Shih, H. P., Evolution of microstructure of AISI 304 stainless steel joint brazed by mechanically alloyed nickel base filler with different silicon content, *Journal of Materials Science Letters, 22* (2003), 1, pp. 79-82

Received: 24.11.2024.
Revised: 18.02.2025.
Accepted: 17.03.2025.